Atmos. Chem. Phys., 11, 5485–5490, 2011
www.atmos-chem-phys.net/11/5485/2011/
doi:10.5194/acp-11-5485-2011

Atmospheric Chemistry and Physics

Tropopause height at 78° N 16° E: average seasonal variation 2007–2010

C. M. Hall[1], G. Hansen[2], F. Sigernes[3], and K. M. Kuyeng Ruiz[4]

[1]Tromsø Geophysical Observatory, University of Tromsø, Norway
[2]Norwegian Institute for Air Research, Tromsø, Norway
[3]The University Centre in Svalbard, Longyearbyen, Norway
[4]Jicamarca Radio Observatory, Lima, Peru

Received: 25 October 2010 – Published in Atmos. Chem. Phys. Discuss.: 4 January 2011
Revised: 12 April 2011 – Accepted: 6 June 2011 – Published: 15 June 2011

Abstract. We present a seasonal climatology of tropopause altitude for 78° N 16° E derived from observations 2007–2010 by the SOUSY VHF radar on Svalbard. The spring minimum occurs one month later than that of surface air temperature and instead coincides with the maximum in ozone column density. This confirms similar studies based on radiosonde measurements in the arctic and demonstrates downward control by the stratosphere. If one is to exploit the potential of tropopause height as a metric for climate change at high latitude and elsewhere, it is imperative to observe and understand the processes which establish the tropopause – an understanding to which this study contributes.

1 Introduction and data sources

It is now a well-established fact that trace gases determining the greenhouse effect in the troposphere have increased drastically in recent decades, causing a noticeable warming on global scale in the troposphere (Solomon et al., 2007 and references therein). It is not so commonly known that the very same increases in greenhouse gases (GHG) that are responsible for global warming in the troposphere are also responsible for a cooling of the middle atmosphere (e.g. Rishbeth and Roble, 1992; Rishbeth and Clilverd, 1999; Roble and Dickenson, 1989). Indeed, the absolute expansion of the troposphere combined with contraction of the middle atmosphere leads to a net contraction and therefore lowering of pressure levels in the ionosphere and the ionospheric layers associated with them (e.g. Ulich and Turunen, 1997; Hall et al., 2007). Intuitively, a warming and expansion of the troposphere will result in an upward displacement of the tropopause; a cooling of the lower stratosphere, whatever the cause, will also result in an upward displacement. Thus if GHG concentration increases alone are responsible for these temperature changes, tropopause height change should represent a more sensitive metric than, for example surface air temperature. Such responses of the tropopause to control from above and below and the potential as a metric for climate change are discussed by, for example, Santer et al. (2003) and Zängl and Hoinka (2001). Obviously, if we are to exploit the tropopause altitude for climate study, we need to fully understand the controlling mechanisms (e.g. Hu et al., 2010). However, one also has to consider systematic changes of atmospheric dynamical patterns as a potential cause of tropopause altitude and temperature changes, and much of the research on the Upper Troposphere/Lower Stratosphere (UTLS) regions focuses on this issue (see, e.g., SPARC Newsletter no. 35, p. 8–13, 2010). While interest to some degree has moved from the tropical to the extratropical UTLS region (e.g. Bègue et al., 2010), the polar regions, reviewed by e.g. Highwood et al. (2000), are still poorly covered.

At 78° N 16° E (Adventdalen, Svalbard) the SOUSY VHF radar continually monitors the tropopause location, the radar system itself and subsequent analysis technique for identifying the radar tropopause being fully described by Hall et al. (2009). The radar tropopause (e.g. Gage and Green, 1979) and its relation to the meteorological tropopause (e.g. WMO, 1996), typified by a systematic height difference, are discussed by Röttger and Hall (2007) and Hall et al. (2009), and we shall investigate this further in this study. The radar tropopause is approximately 2 km above

Correspondence to: C. M. Hall
(chris.hall@uit.no)

the meteorologically defined tropopause (as we shall see in Fig. 3). The effective radar cross section at VHF is proportional to the square of the mean gradient of the refractive index; this in turn being proportional to the square of the Brunt-Väisälä frequency which depends linearly on the potential temperature gradient. In effect this directly implies that one expects a maximum in echo power corresponding to the maximum in temperature gradient, this normally occurring in the lower stratosphere, somewhat above the meteorological tropopause defined as the lowest level at which the lapse rate decreases to $2\,\mathrm{K\,km^{-1}}$ or less, provided that the average lapse rate between this level and all higher levels within 2 km does not exceed $2\,\mathrm{K\,km^{-1}}$.

Daily average radar tropopause heights are obtained from the original hourly values providing an almost uninterrupted time-series since November 2007. In addition we shall make use of surface air temperatures obtained at the nearby Kjell Henriksen Observatory (KHO) approximately 2 km SE of the radar at an altitude of 520 m on Breinosa, and also the total ozone column density climatology measured at Ny Ålesund approximately 120 km to the NW. Surface air temperatures were originally recorded at 5 min intervals, but here we use daily means. The station consists of a standard Campbell Scientific data logger with sensors for pressure, wind and temperature, and is part of the network of weather stations that The University Centre in Svalbard (UNIS) operates in the surroundings of Longyearbyen. The data are ported to the main observatory (KHO) in real time. The ozone column density monthly climatology is derived from the (fragmentary) time-series from 1950 to 2007, including the historical Dobson measurements from Longyearbyen 1950–1968, re-analyzed and published by Vogler et al. (2006), satellite observations from the time period 1970–2005 (BUV 1970–1977, TOMS 1979–2005), and measurements by means of the SAOZ instrument (since 1991) and the GUV filter instrument (since 1995) in Ny-Ålesund.

2 Results

The daily values obtained from the original hourly tropopause height determinations are shown in Fig. 1 together with the result of applying a 30-day Lee filter (Lee, 1986) this method (more traditionally used in image processing) being particularly useful for removing outliers which would otherwise influence the result had boxcar smoothing been used. The result helps to illustrate the seasonal variation: a minimum in early April, a summer maximum and a secondary winter peak. If we then form monthly averages to obtain a seasonal climatology for the years 2008 to 2010 inclusive we arrive at Fig. 2. Here the radiosonde-determined meteorological tropopause from Ny Ålesund (Koldewey Station of the Alfred Wegener Institute) from the period November 2008 to November 2008 inclusive is also shown together with the WMO (1996) model. The numbers on the radar-

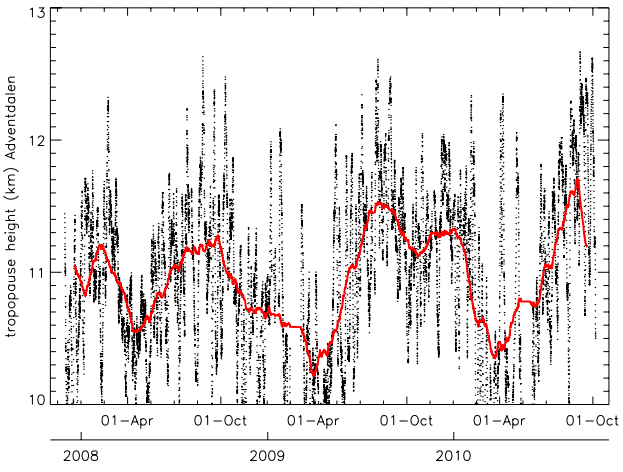

Fig. 1. Tropopause heights (radar tropopause) since November 2007, as determined by SOUSY. Daily medians of hourly values are indicated by black dots; thick solid line shows result of applying a 30-day Lee-filter.

measurement standard deviation bars indicate the numbers of hourly values that contribute to each monthly value. Again we see the clear April minimum followed by a summer maximum and secondary winter maximum. The WMO model shows a similar signature of primary and secondary maxima and minima, but these only agree approximately with the observations, thus illustrating room for updating the model, at least for this geographic location. We see a good agreement in seasonal variation between radar and radiosonde measurements and also the systematic height difference between meteorological and radar determinations, as mentioned earlier. This is now shown in the upper panel of Fig. 3: there is a distinct seasonal variation but with a peak-to-peak magnitude of only 1 km., the significance of which is perhaps arguable considering the combined standard deviations (indicated in the figure) in the monthly means from each measurement. Nevertheless, we have performed a linear regression (Fig. 3, middle panel) resulting in the approximate relation:

$$\text{radar-tropopause} = 5.4 \pm 0.4\,\text{km} + 0.62 \pm 0.05 \times \text{meteorological-tropopause} \quad (1)$$

where the above uncertainties are the 1-sigma errors in the regression and the 95 % confidence intervals are shown by dotted lines in the figure. By applying this conversion to the radar determination it is therefore possible to estimate the meteorological tropopause altitude as we illustrate in the bottom panel of Fig. 3 (line width indicates the uncertainties based on those of the linear regression).

Having reiterated the agreement in seasonal variation between radiosonde and radar determinations that was established earlier by Hall et al. (2009), and also quantified the relationship between altitudes discussed by Röttger and Hall (2007), we turn our attention to comparison with surface

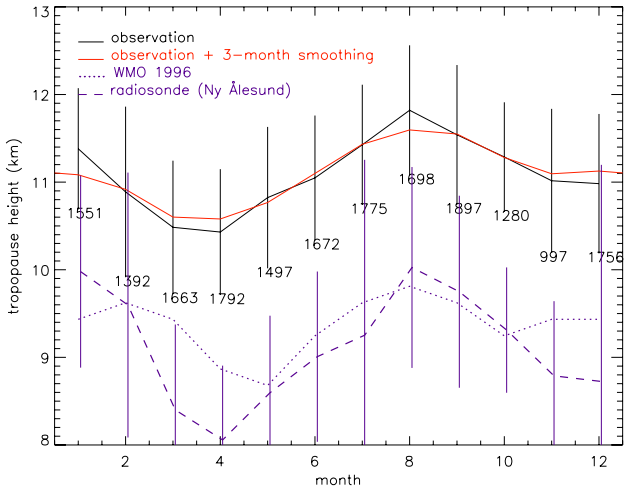

Fig. 2. Monthly values of tropopause height. The upper black line shows the monthly climatology for the period 2008–2010 inclusive as determined by radar, the vertical bars indicating the standard deviation and the numbers showing the number of hourly values used for each point. The overlying smooth line shows a 3-month Lee filter smoothing to illustrate the mid-winter weak secondary maximum. The WMO 1996 model is indicated by the dotted line, while the dashed line shows the corresponding values obtained from radiosonde measurements at Ny Ålesund, 120 km to the NW of the radar (standard deviation bars are very slightly offset for clarity).

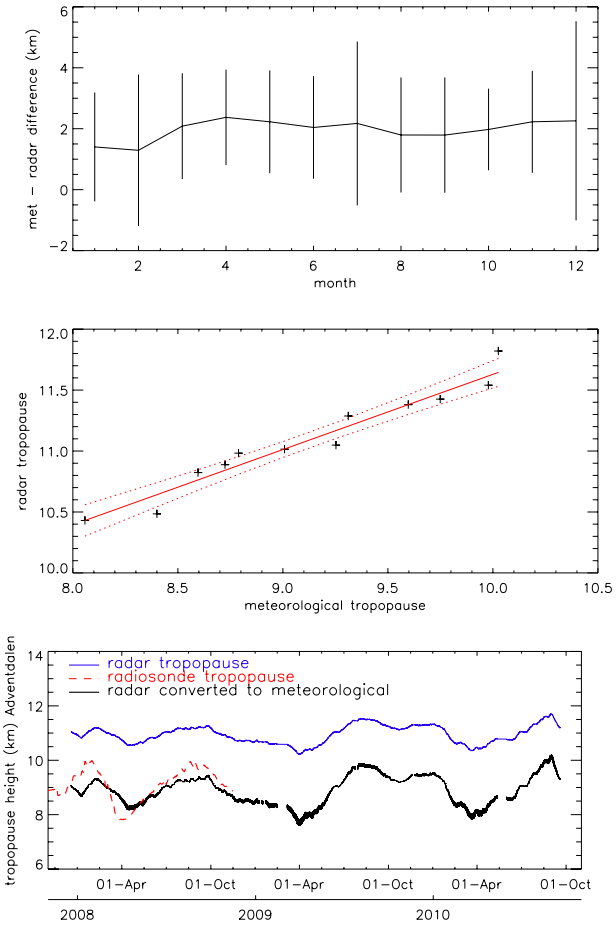

Fig. 3. Upper panel: the height difference between radar and radiosonde tropopause determinations. Although showing a distinct seasonal variation, the peak to peak magnitude is only 1 km. Vertical bars indicate standard deviations corresponding to the monthly means. Middle panel: linear regression of radar tropopause on meteorological tropopause heights (+) together with 95 % confidence limits (dotted hyperbolae). Bottom panel: tropopause determinations for the period of observation with 30-day Lee filter applied for clarity. Thin upper line: radar determination; lower dashed line: radiosonde determination; solid thick line: estimate the meteorological tropopause (uncertainties based on those of the regression indicated by line thickness).

air temperature. Monthly averages are compared using cross correlations as shown in the upper panel of Fig. 4. This figure is an updated version of the one shown earlier by Hall et al. (2009) but incorporating the newer radar data, and includes results of comparing (a) the previous SOUSY radar (e.g. Röttger and Hall, 2007) with temperatures distributed by the Norwegian Meteorological Institute, *met.no*, from Longyearbyen airport 12 km NW of the radar, (b) the current SOUSY radar with temperatures measured in Adventdalen (5 km NW of the radar) and (c) radiosonde measurements with Adventdalen temperatures. The rationale for including data from so many sources was to consciously employ quite independent measurements. As can be seen, the temperature variation leads that of the tropopause height by one month; inclusion of newer data from SOUSY does not alter the conclusion of Hall et al. (2009). If we now employ daily values rather than monthly averages, and now using only temperatures from Breinosa, the same result emerges, as shown in the lower panel of Fig. 4. The maximum correlation is where the temperature variation leads that of the tropopause height by approximately one month. By smoothing the radar tropopause heights with a 30 day Lee filter prior to the correlation analysis we obtain a coefficient of 0.8 at a lag of 33 days. By first correlating with daily radar tropopause values and then smoothing with a 30-day Lee filter we obtain a coefficient of 0.35 at a lag of 27 days. Using daily values only, the correlation maximizes at 0.4, again at a lag of 33 days, although a secondary peak is evident at zero lag corresponding to the somewhat earlier tropopause height minimum in 2010 (this is seen in Fig. 1 but disappears with smoothing as seen in Fig. 3). Again we confirm the conclusion of Hall et al. (2009), that the spring tropopause height minimum lags that of the surface air temperature by approximately one month.

One would expect prima facie, that the meteorological tropopause height, essentially being the temperature minimum between the adiabatic tropopause and the region of positive temperature gradient of the lower stratosphere, is

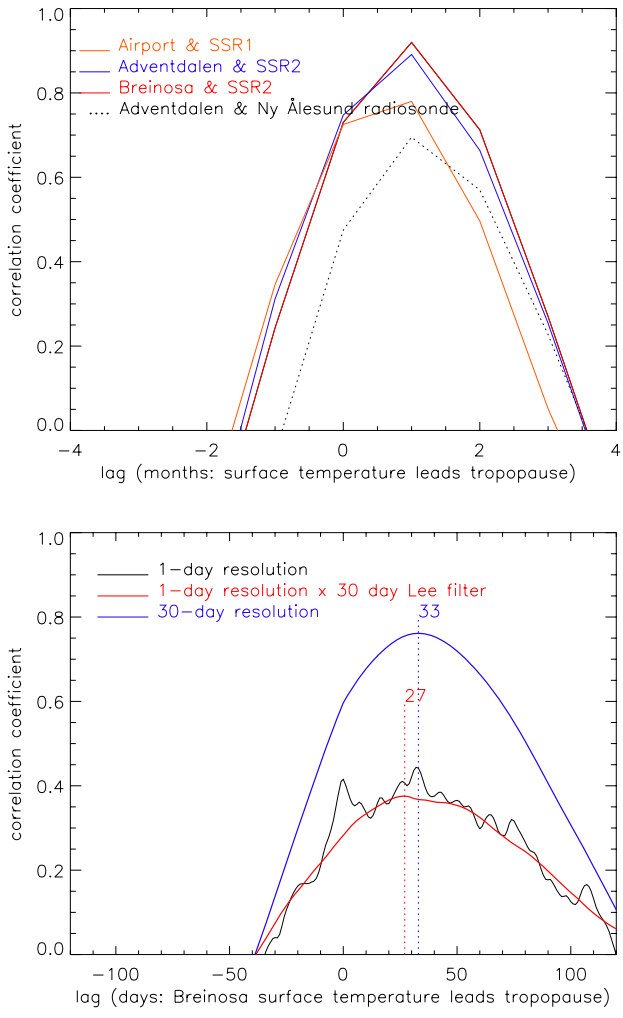

Fig. 4. Upper panel: updated version of results from Hall et al. (2009) showing correlations between tropopause determinations and temperature measurements (see text and Hall et al. (2009) for details. Lower panel: correlations based on daily data (variable line), 30-day smoothed correlation (smooth lower line), and correlation between daily temperature and 30-day smoothed tropopause height (upper smooth line). All temperatures from Breinosa.

a reflection of the troposphere thickness. Given a constant lapse rate through the troposphere and ignoring boundary layer inversions, variations in tropospheric thickness and therefore tropopause height could be expected to occur simultaneously with surface temperature variation. While troposphere temperature does indeed strongly influence the tropopause altitude, it is not, however the only governing factor as both the ozone concentration in the stratosphere and the solar UV flux vary strongly with season, particularly at high latitude. In spring, breakdown of the polar vortex gives rise to entrainment of ozone in the polar cap and around the same time (depending on latitude), solar flux increases suddenly as the polar night ends. The resulting heating of the stratosphere tends to displace the tropopause downwards competing with the onset of spring warming and expansion of the troposphere (e.g. Highwood et al., 2000). The effects of tropospheric warming and stratospheric ozone content on tropopause altitude are discussed by, for example, Santer et al. (2003). Thus in our final comparison we shall examine the relation between tropopause height and total column ozone density monitored 120 km NW of the radar. We reproduce the tropopause data shown earlier in Fig. 2 in the upper panel of Fig. 5. The middle panel shows the total column ozone monthly climatology (means and standard deviations) in Dobson units as described in the Introduction. In the bottom panel of the figure we show the monthly climatology (means and standard deviations) of surface air temperature at Breinosa since November 2007. From the temperature data we can see the late winter minimum in March occurring where radiative cooling is in equilibrium with solar warming, signifying the end of the arctic winter; this precedes both the minimum in tropopause height and maximum in ozone column density by approximately one month. Similarly, and also contributing to the lag between seasonal variations of tropopause height and surface air temperature, the maximum summer temperature occurs in July, as opposed to the maximum tropopause height which occurs in August. During the autumn, the air cools and there is a corresponding fall in tropopause suggesting less downward control by the stratosphere from September to November. During Autumn, the ozone suffers a dramatic depletion; there is also an absence of solar UV during the polar night and the virtual absence of stratospheric heating competes with radiative cooling of the troposphere, possibly contributing to the secondary maximum in tropopause height in December–January. These effects are also illustrated in Fig. 6. Here we show the complete time series of derived meteorological tropopause based on radar data and the preceding regression analysis, the corresponding surface air temperatures from Breinosa and the corresponding ozone column densities based on the monthly climatology (shown in Fig. 5). Clearly, the tropopause variation is complex compared to those of ozone column density and surface air temperature and longer time series combined with other tropospheric parameters (e.g. 500 hPa temperatures) and stratospheric parameters (e.g. temperatures and polar vortex dynamics) will be required in future studies of this kind.

3 Conclusions

Earlier Hall et al. (2009) demonstrated the capability of the SOUSY VHF radar on Svalbard for monitoring of tropopause altitude, and here we employ data acquired since. We examine the relationship between the radar and meteorological tropopause and tentatively quantify it, but most importantly validating the initial results with the newest data. We present predictions of the meteorological tropopause

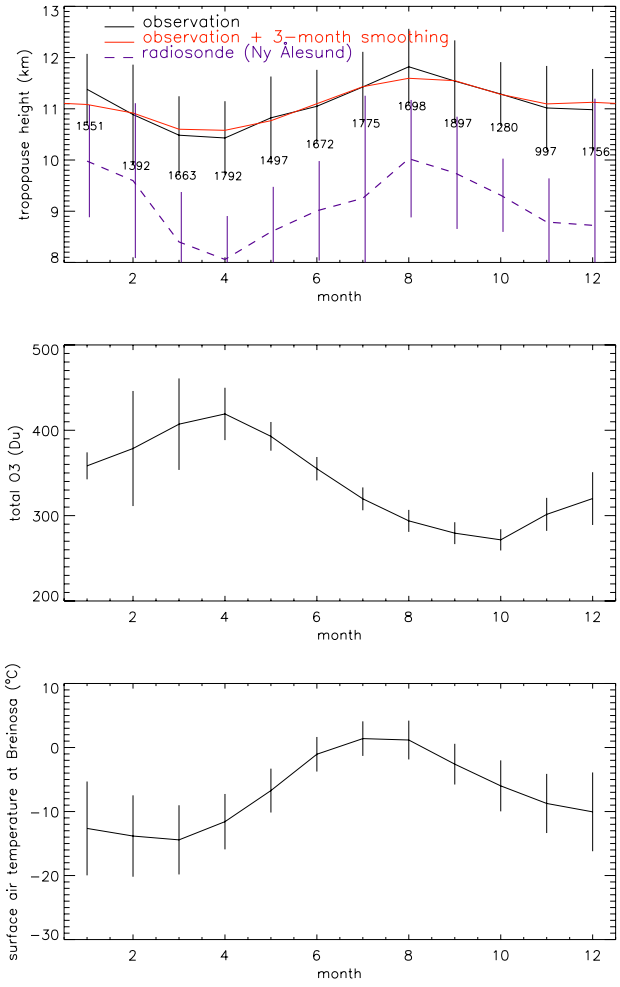

Fig. 5. Upper panel: repetition of Fig. 2, but included here to show seasonal variation in the contexts of those of ozone and temperature. Middle panel: monthly climatology of total column O_3 in Dobson units, as measured at Ny Ålesund. Bottom panel: monthly climatology of surface air temperature at Breinosa. Vertical bars indicate standard deviations corresponding to the monthly means; in the upper panel numbers on the standard deviation bars indicate the numbers of tropopause determinations used in each mean.

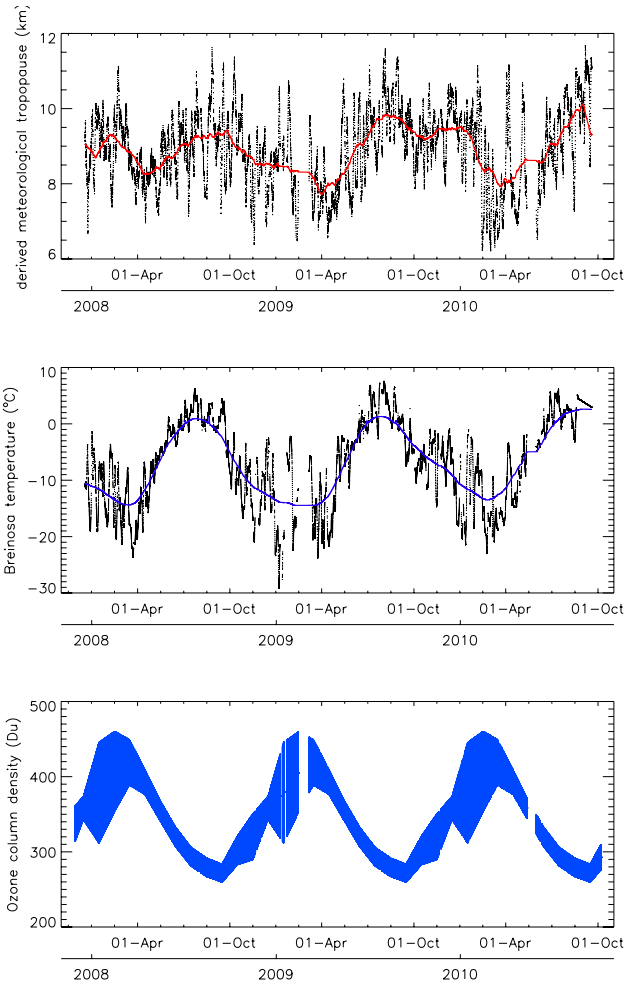

Fig. 6. Upper panel: final estimate of meteorological tropopause derived from radar data (daily medians of hourly measurements in black, overlaid by 30-day Lee-filtered version in red). Middle panel: surface air temperature at Breinosa (daily means in black, overlaid by 30-day Lee-filtered version in blue). Bottom panel: corresponding daily means of ozone column density with line width indicating standard deviation.

altitude based on the radar data and compare this with temperature and ozone column density, summarized as monthly and daily means in Figs. 5 and 6. That the surface air temperature seasonal variation leads that of tropopause height by approximately one month, a tentative result of Hall et al. (2009), is also confirmed here. Moreover examination of ozone column density reveals a coincidence of the spring ozone maximum with the tropopause altitude minimum. Thereafter, the tropopause gains height during the summer coinciding with increases in troposphere temperature and gradual decrease in ozone. The autumn/winter ozone depletion characterized by a minimum in October precedes a weak secondary increase in tropopause altitude, typically in mid-winter. These secondary increases resulted in distinct peaks in early 2008 and 2010, but only as a weak increase in 2009. Although longer time series will be required to confirm it, one could hypothesize this is a QBO influence from mid-latitude. While we have worked with ozone column density here, Hansen and Svenøe (2005) demonstrated a strong correlation between total ozone and 50 hPa temperature at Tromsø, based on 60 yr of data. Thus we find that the tropopause is controlled both by tropospheric and stratospheric temperatures, the latter being determined by a complex combination of the Brewer-Dobson circulation (e.g. Salby, 1996) and solar UV flux. Indeed the tropopause is likely to be determined by several interacting processes. The radar position is, on average within the footprint of the winter

stratosphere polar vortex (e.g. Manney and Sabutis, 2000) and the seasonal variation we observe can be expected to reflect this. All mechanisms controlling the tropopause location exhibit particularly strong seasonal variations at high latitude; this study contributes to our understanding of these mechanisms – necessary if we are to employ tropopause altitude as a metric for climate change.

Acknowledgements. The authors would like express gratitude for the help and support of the Jicamarca staff, in particular the members of the Electronics and Instrumentation group, and Jürgen Röttger. We thank the Alfred Wegener Institute, in particular Marion Maturilli, for tropopause data from their Ny Ålesund station. Temperature data from Longyearbyen airport have been provided by the Norwegian Meteorological Institute. We also acknowledge the occasional maintenance of the SSR by the staff of the EISCAT Svalbard Radar.

Edited by: W. Ward

References

Bègue, N., Bencherif, H., Sivakumar, V., Kirgis, G., Mze, N., and Leclair de Bellevue, J.: Temperature variability and trends in the UT-LS over a subtropical site: Reunion (20.8° S, 55.5° E), Atmos. Chem. Phys., 10, 8563–8574, doi:10.5194/acp-10-8563-2010, 2010.

Gage, K. S. and Green, J. L.: Tropopause detection by partial specular reflection with very-high-frequency radar, Science, 203, 1238–1240, doi:10.1126/science.203.4386.1238, 1979.

Hall, C. M., Brekke, A., and Cannon, P. S.: Climatic trends in E-region critical frequency and virtual height above Tromsø (70° N, 10° E), Ann. Geophys., 25, 2351–2357, doi:10.5194/angeo-25-2351-2007, 2007.

Hall, C. M., Röttger, J., Kuyeng, K., Sigernes, F., Claes, S., and Chau, J. L.: Tropopause altitude detection at 78° N, 16° E, 2008: first results of the refurbished SOUSY radar, Radio Science, 44, RS5008, doi:10.1029/2009RS004144, 2009.

Hansen, G. and Svenøe, T.: Multilinear regression analysis of the 65-year Tromsø total ozone series, J. Geophys. Res., 110, D10103, doi:10.1029/2004JD005387, 2005.

Highwood, E. J., Hoskins, B. J., and Berrisford, P.: Properties of the arctic tropopause, Q. J. Roy. Meteorol. Soc., 126, 1515–1532, 2000.

Hu, Y., Xia, Y., and Fu, Q.: Tropospheric temperature response to stratospheric ozone recovery in the 21st century, Atmos. Chem. Phys. Discuss., 10, 22019–22046, doi:10.5194/acpd-10-22019-2010, 2010.

Lee, J. S.: Speckle suppression and analysis for synthetic aperture radar images, Opt. Eng., 25, 636–643, 1986.

Manney, G. L. and Sabutis, J. L.: Development of the polar vortex in the 1999–2000 Arctic winter stratosphere, Geophys. Res. Lett., 27, 2589–2592, 2000.

Rishbeth, H. and Clilverd, M.: Long-term change in the upper atmosphere, Astronomy and Geophysics, 40, 3.26–3.28, 1999.

Rishbeth, H. and Roble, R. G.: Cooling of the upper atmosphere by enhanced greenhouse gases – modelling of thermospheric and ionospheric effects, Planet. Space Sci., 40, 1011–1026, 1992.

Roble, R. G. and Dickinson, R. E.: How will changes in carbon-dioxide and methane modify the mean structure of the mesosphere and thermosphere?, Geophys. Res. Lett., 16, 1441–1444, 1989.

Röttger, J. and Hall, C. M.: Climatology of the radar tropopause over Svalbard 2005 and 2006, Proceedings MST-11 workshop India 2006, ISBN 10:0230-63414-1, 726–729, 2007.

Salby, M. L.: Fundamentals of Atmospheric Physics, Academic Press, San Diego, California, 627 pp., ISBN 0-12-615160-1, 1996.

Santer, B. D., Sausen, R., Wigley, T. M. L., Boyle, J. S., AchutaRao, K., Doutriaux, C., Hansen, J. E., Meehl, G. A., Roeckner, E., Ruedy, R., Schmidt, G., and Taylor, K. E.: Behavior of tropopause height and atmospheric temperature in models, reanalyses, and observations: Decadal changes, J. Geophys. Res., 108(D1), 4002, doi:10.1029/2002JD002258, 2003.

Solomon, S., Qin, D., Manning, M., Chen, Z., Marquis, M., Averyt, K. B., Tignor, M., and Miller, H. L. (Eds.): Contribution of Working Group I to the Fourth Assessment Report of the Intergovernmental Panel on Climate Change, 996 pp., Cambridge University Press, Cambridge, United Kingdom and New York, NY, USA, 2007.

Ulich, T. and Turunen, E.: Evidence for long-term cooling of the upper atmosphere in ionosonde data, Geophys. Res. Lett., 24, 1103–1106, 1997.

Vogler, C., Brönnimann, S., and Hansen, G.: Re-evaluation of the 1950–1962 total ozone record from Longyearbyen, Svalbard, Atmos. Chem. Phys., 6, 4763–4773, doi:10.5194/acp-6-4763-2006, 2006.

WMO: Measurements of upper air temperature, pressure, and humidity, Guide to Meteorological Instruments and Methods of Observation, 6th ed., WMO I.12-1–I.12-32, 1996.

Zängl, G. and Hoinka, K. P.: The tropopause in polar regions, J. Climate, 14, 3117–3139, 2001.